ФІЗИКА І ХІМІЯ ТВЕРДОГО ТІЛА
Т. 12, № 3 (2011) С. 579-584

PHYSICS AND CHEMISTRY OF SOLID STATE
V. 12, № 3 (2011) P. 579-584

PACS 621.382.2

ISSN 1729-4428

E.F. Venger[1], A.I. Ievtushenko[2], L.Yu. Melnichuk[2], A.V. Melnichuk[2]

Surface Polaritons in 6H-SiC Single Crystals Placed in a Strong Uniform Magnetic Field

[1]V. Lashkaryov Institute of Semiconductor Physics, NAS Ukraine,41 Prospect Nauky, Kyiv 03028, Ukraine, e-mail: venger@isp.kiev.ua
[2]Mykola Gogol State Pedagogic University, 2 Kropyv'yans'kogo St., Nizhyn 16600, Ukraine, e-mail: mov310@mail.ru

We demonstrate a feasibility of excitation of surface phonon and plasmon-phonon polaritons (PPPs) in optically anisotropic silicon carbide single crystals (polytype 6H) placed in a strong uniform magnetic field, at orthogonally related optical axis, wave vector and magnetic field: $C\|x$, $K\|C$, $xy\|C$; $C\|z$, $K \perp C$, $xy \perp C$; $C\|y$, $K \perp C$, $xy\|C$, $\vec{H} \perp K$, $\vec{H}\|y$. The attenuated total reflectance spectra were registered, and the main PPP properties (dispersion curves and damping coefficient) in 6H-Sic single crystal subjected to action of strong uniform magnetic field were studied. The effect of a uniform magnetic field on the properties of PPs in 6H-SiC was determined.

Key words: surface polaritons, anisotropy, magnetic field, dispersion curves, silicon carbide.

Стаття поступила до редакції ; прийнята до друку 15.06.2011.

Introduction

Investigations of the properties of surface polaritons (SPs) in optically-isotropic and optically-anisotropic media make a complicated problem that remains actual up to now [1 – 5]. Of special importance are, in particular, uniaxial polar optically-anisotropic silicon carbide single crystals (polytype 6H). They are studied extensively bearing in mind fundamental as well as applied aspects [6 – 10]. The 6H-SiC single crystals belong to the wurtzite structure; their spatial symmetry group is C_{6V}^4 ($P6_3mc$). They demonstrate high anisotropy of the plasma system properties [7]. Anisotropy of electron effective mass as well as phonon and plasmon damping coefficients in 6H-SiC were studied in [8]. The main properties of plasmon-phonon polaritons (PPPs) in 6H-SiC single crystals at mutually orthogonal orientations and various degrees of doping were investigated in [9]. The authors of [10, 11] have detected and studied, for the first time, some novel types of surface PPPs (SPPPs) in doped anisotropic 6H-SiC single crystals at the following orientations of SPPP wave vector *K* and crystal surface *xy* relative to the crystal optical axis *C*: $K \perp C$, $xy \perp C$. However, up to now, there are no data in the literature concerning investigations of concurrent effect of anisotropy of both plasma and phonon subsystems and uniform magnetic field on the properties of SPs in 6H-SiC.

In this work, we studied the properties of surface phonon and plasmon-phonon polaritons in silicon carbide crystals (polytype 6H) placed in a uniform magnetic field $\vec{H}$ up to 100 kOe ($\vec{H} \perp K$, $\vec{H}\|y$) at three mutually orthogonal orientations of crystal optical axis and wave vector: $C\|x$, $K\|C$, $xy\|C$; $C\|z$, $K \perp C$, $xy \perp C$; $C\|y$, $K \perp C$, $xy\|C$.

I. Samples and experimental procedure

The experimental attenuated total reflectance (ATR) spectra of 6H-SiC single crystals were taken in the 400−1400 cm^{-1} range with a spectrometer ИКС-29 and ATR attachment НПВО-2. The angle of incidence range for IR radiation that hit an ATR element was from 20 up to 60°, while the accuracy of angle setting was no worse than 6′. A gap between the semicylinder and 6H-SiC single crystal under investigation was set using calibrated fluoroplastic spacers. We used an ATR element 12 mm in diameter; its refractive index was 2.38.

II. Results and discussion

Let us consider an optically-anisotropic uniaxial polar semiconductor (in our case, 6H-SiC) bordering an optically-isotropic medium (air). The SPs are excited and

propagate along the *x*-axis lying in the single crystal surface (*xy*-plane). A uniform magnetic field is parallel to the surface studied and normal to the wave vector (the Voigt configuration). The ATR coefficient was calculated for the orientation C||x, C||y, C||z according to the procedure described in [7]. The permittivity of a 6H-SiC single crystal placed in a uniform magnetic field is [13]

$$\begin{pmatrix} \varepsilon_1 & i\varepsilon_2 & 0 \\ -i\varepsilon_2 & \varepsilon_1 & 0 \\ 0 & 0 & \varepsilon_3 \end{pmatrix}, \qquad (1)$$

where

$$\varepsilon_1 = \varepsilon_\infty \left(1 + \frac{\nu_L^2 - \nu_T^2}{\nu_T^2 - \nu^2 - i\gamma_f \nu} + \frac{\nu_p^2 \left(\nu + i\gamma_p \right)}{\nu \left(\Omega^2 - \left(\nu + i\gamma_p \right)^2 \right)} \right),$$

$$\varepsilon_2 = \frac{\varepsilon_\infty \nu_p^2 \Omega}{\nu \left(\left(\nu + i\gamma_p \right)^2 - \Omega^2 \right)}, \qquad (2)$$

$$\varepsilon_3 = \varepsilon_\infty \left(1 + \frac{\nu_L^2 - \nu_T^2}{\nu_T^2 - \nu^2 - i\gamma_f \nu} - \frac{\nu_p^2}{\nu \left(\nu + i\gamma_p \right)} \right),$$

Here $\varepsilon_{\infty \perp,\parallel}$ is the high-frequency permittivity parallel and perpendicular to the optical axis *C*; $\nu_{L \perp,\parallel}$, $\nu_{T \perp,\parallel}$ are, correspondingly, the frequencies of longitudinal and transverse optical phonons perpendicularly and parallel to the crystal axis; $\nu_{p \perp,\parallel}$ is the frequency of plasma resonance perpendicular and parallel to the crystal axis; $\gamma_{p \perp,\parallel}$ is the plasmon damping coefficient perpendicular and parallel to the crystal axis; $\gamma_{f \perp,\parallel}$ is the optical phonon damping coefficient perpendicular and parallel to the crystal axis; $\Omega = \frac{eH}{mc}$ is the cyclotron frequency.

Figure 1 presents the experimental ATR spectra (○) of 6H-SiC single crystal (sample ПСЕ-3Б) for orientation C||z, K ⊥ C, xy ⊥ C as well as calculated curves for the orientations C||x, K||C, xy||C (curve 1); C||z, K ⊥ C, xy ⊥ C (curve 2) and C||y, K ⊥ C, xy||C (curve 3) without action of magnetic field on the semiconductor. The angle of incidence on the ATR prism is 40°. The spacing between the sample under investigation and prism was, correspondingly, 3.1 (1), 2.7 (2) and 2.5 (3) μm. The curves 1′–3′ were calculated

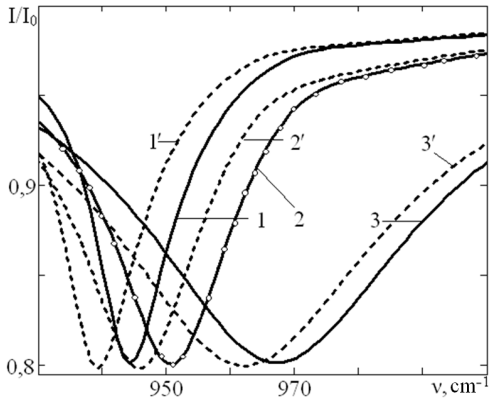

Fig. 1. ATR spectra of 6H-SiC (sample ПСЕ-3Б).

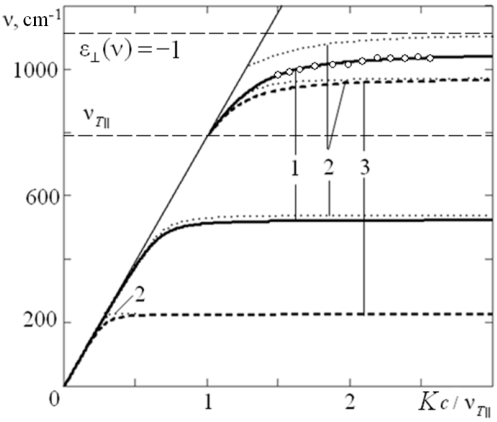

Fig. 2. High- and low-frequency dispersion branches in 6H-SiC (sample SC-2).

for the case of action of 100 kOe magnetic field (orientation $\vec{H} \perp K$, $\vec{H} \| y$) on the 6H-SiC single crystal. The curves 1 – 3 coincide with the corresponding curves 1′–3′; therefore, the latter are shifted in the plot towards lower frequencies by 5 cm^{-1}. The frequencies corresponding to the minima of ATR spectra are 944 (1, 1′), 951 (2, 2′) and 967 (3, 3′) cm^{-1}, respectively; the spectrum half-widths are 16 (1, 1′), 26 (2, 2′) and 54 (3, 3′) cm^{-1}, respectively. One can see from Fig. 1 that strong magnetic field, at the orientation indicated, practically does not change the ATR spectra of 6H-SiC single crystal.

The results of investigations made in [7 – 11] showed that excitation of SPs of phonon- and plasmon-phonon-types in 6H-SiC occurs in the neighborhood of the transverse and longitudinal optical phonon frequencies. There are minima in the ATR spectra. According to [7, 13], the frequencies of minima correspond to the surface modes n^+ and n^- at $H \approx 0$ and pseudo-surface modes at higher fields. It is evident that the surface modes in 6H-SiC single crystal coincide with the pseudo-surface ones. As the cyclotron frequency approaches the frequency of surface excitations, magnetic field complicates considerably the dispersion relations. This is because (i) the diagonal components of permittivity tensor are not equal to each other and (ii) off-diagonal components of permittivity tensor appear in

Table 1

Dispersion relations for uniaxial crystal placed in magnetic field ($\vec{H} \perp K$, $\vec{H} \| y$) at three orientations

Orientations	C‖z	C‖x	C‖y
Dispersion relations	$K^2 = \varepsilon_{v\|\|} \frac{1-\varepsilon_{v\perp}}{1-\varepsilon_{v\perp}\varepsilon_{v\|\|}}$	$K^2 = \varepsilon_{v\perp} \frac{1-\varepsilon_{v\|\|}}{1-\varepsilon_{v\perp}\varepsilon_{v\|\|}}$	$K^2 = \frac{\varepsilon_{v\perp}}{1+\varepsilon_{v\perp}}$

magnetic field. The corresponding equations are presented in Table 1.

Shown in Fig. 2 are the experimental dispersion curves (○) for orientation C‖z, $K \perp C$, $xy \perp C$ and calculated dispersion curves (lines) for orientations C‖y, $K \perp C$, xy‖C (1); C‖z, $K \perp C$, $xy \perp C$ (2); and C‖x, K‖C, xy‖C (3) in the case of no magnetic field (sample SC-2). One can see that, if the optical axis C‖y (i.e., is perpendicular to the propagation direction and to the normal to crystal surface), then there are two dispersion branches. The lower branch, n^-, exists in the whole range of wave vector K variation. As to the upper branch, n^+, its domain of existence is limited by the condition $K > w_{T\perp,\|}/c$. If the crystal optical axis is perpendicular to the surface (C‖z) or parallel to the propagation direction (C‖x), then the number of dispersion branches increases and may become as big as five. One of them is an analog to the low-frequency branch n^-; it begins under the condition $K = 0$. The number of branches existing at $K > w_{T\|}/c$, $w_{T\perp}/c$, varies depending on orientation of the crystal optical axis relative to the crystal surface. The above modes may be excited over the whole range of K variation (similarly to the case of optically-isotropic crystal) or in the bounded above interval [10, 11].

It was shown in [13] that surface waves remain their *TM*-type in the Voigt geometry only. Magnetic field *H* is perpendicular to the plane of polarization of surface wave, xz, in which its electric vector rotates. Cyclotron motion of electrons also takes place in that plane. This motion coincides with the "proper" rotation of the electric vector of surface wave at one sign of *H*, while at reverse sign of *H*, the cyclotron motion is opposite to it. This is the reason for nonequivalence of the $+K$ and $-K$ directions; the frequencies that correspond to different orientations of *H* become different too.

Our investigations of dispersion curves in 6H-SiC single crystals placed in strong (100 kOe) magnetic field ($\vec{H} \perp K$, $\vec{H} \| y$) at three mutually orthogonal orientations indicated essential distinctions in their behavior at orientation variations. To illustrate, at orientation C‖y, $K \perp C$, xy‖C without magnetic field (sample ПСЕ-3Б), there exist two dispersion curves (see curves 1 and 2 in Fig. 3). The limiting n_s value is determined from the equation $e_\perp(n) = -1$. Under action of magnetic field of 100 kOe, the dispersion curves change (see curves $1'-3'$). One can see from Fig. 3 that the high-frequency dispersion curve does not change in magnetic field, while the low-frequency one shifts towards bigger wavelengths. An additional dispersion branch (referred to as a "virtual" mode in [13]) appears in the 500–550 cm^{-1} frequency range. Its properties are similar to those of surface oscillations of type II in anisotropic crystals [14]. However, it was shown in [15] that zinc oxide single crystals (contrary to 6H-SiC) demonstrate strong anisotropy of the properties of their phonon subsystem.

Our studies of dispersion curves in 6H-SiC single crystal at orientation C‖x, K‖C, xy‖C showed that the

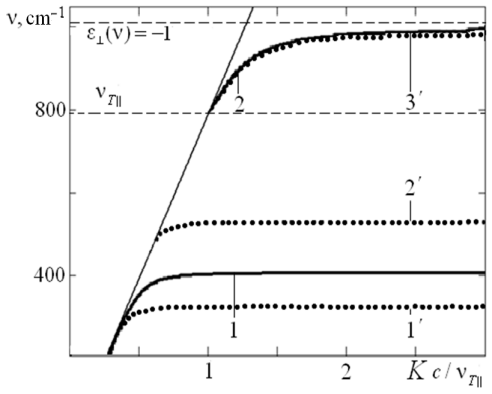

Fig. 3. Dispersion branches in 6H-SiC (sample ПСЕ-3Б) at C‖y, $K \perp C$, xy‖C: 1, 2 − H = 0; $1'-3'$ − H = 100 kOe.

number of dispersion branches at a given orientation remains the same and is two (one high- and one low-frequency branches). The effect of magnetic field on the limiting frequency of the lower dispersion branch is observed in the 162−418 cm^{-1} range. As magnetic field increases from 0 up to 100 kOe, the dispersion branch shifts towards higher frequencies by 256 cm^{-1} (contrary to the case of previous orientation).

Figure 4 presents dispersion curves in heavily doped 6H-SiC (sample ПСЕ-3Б) at orientation C‖z, $K \perp C$, $xy \perp C$. Our calculation indicates possibility to excite (at the above orientation and without magnetic field) up to four dispersion branches (curves 1 − 4). The dots (○) correspond to the experimental data for 6H-SiC. If the 6H-SiC single crystal is exposed to action of magnetic field (H > 50 kOe, $\vec{H} \perp K$, $\vec{H} \| y$), then up to five dispersion branches may be excited in 6H-SiC (curves $1'-5'$). Along with the dispersion curves that have bee studied earlier [10, 11], excitation of a novel branch was detected. Its beginning corresponds to the

Table 2

Limiting frequencies of dispersion branches in 6H-SiC single crystal

SI	H (Oe)	1		$30\cdot10^3$			$65\cdot10^3$			$100\cdot10^3$		
	Sample	n^-_{pf} (cm^{-1})	ν^+_{pf} (cm^{-1})	ν^-_{pf} (cm^{-1})	ν_v (cm^{-1})	ν^+_{pf} (cm^{-1})	ν^-_{pf} (cm^{-1})	ν_v (cm^{-1})	ν^+_{pf} (cm^{-1})	ν^-_{pf} (cm^{-1})	ν_v (cm^{-1})	ν^+_{pf} (cm^{-1})
C‖y												
1.	ПСЕ-3Б	409	998	386	450	997	355	489	996	326	530	995
2.	SC-1	454	1014	432	493	1013	402	529	1011	373	566	1009
3.	SC-2	523	1049	504	558	1048	476	589	1044	449	620	1040
C‖z												
1.	ПСЕ-3Б	162 472	961 1050	279	427	960 1045	18 354	441	958 1046	25 418	468	954 1049
2.	SC-1	170 472	963 1069	298	479	962 1070	16 376	484	957 1072	23 441	507	952 1069
3.	SC-2	225 540	971 1113	347	539	967 1095	21 425	547	960 1097	30 489	564	952 1100
C‖x												
1.	ПСЕ-3Б	162	961	279		960	354		958	418		954
2.	SC-1	170	964	298		962	376		957	441		952
3.	SC-2	225	971	347		967	425		960	489		952

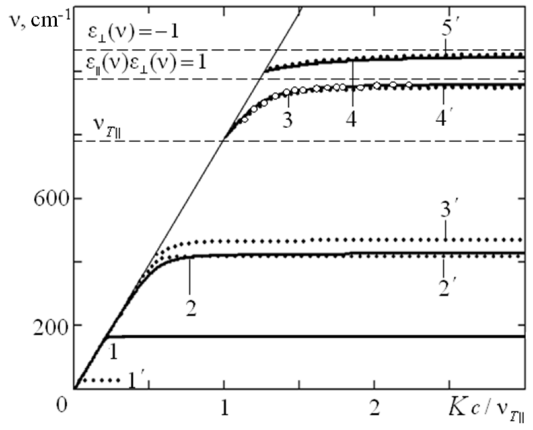

Fig. 4. Dispersion branches in 6H-SiC (sample ПСЕ-3Б) at C‖z , K ⊥ C, xy ⊥ C : 1−4 − H = 0; 1′−5′ − H = 100 kOe.

condition $e_1 = 0$. According to [7], the limiting value n_s is determined from the condition $e_{||}(n)e_{\perp}(n) = 1$, with both $e_{||}$ and $e_{\perp}$ being negative.

Table 2 presents the limiting frequencies of the lower and upper plasmon-phonon as well as "virtual" phonon branches in 6H-SiC single crystals, both without and with action of magnetic field (30, 65 and 100 kOe), at orientations $\vec{H} \perp K$, $\vec{H}$‖y and C‖x, K‖C, xy‖C ; C‖z , K ⊥ C, xy ⊥ C ; C‖y , K ⊥ C, xy‖C .

Figure 5 shows the experimental and theoretical dependences of SP damping coefficient $\Gamma_{sp}(n)$ in 6H-SiC single crystal. The calculations were performed for single crystals with ideally smooth surface [7]. The curves 1–3 were calculated for silicon carbide single crystals with different doping levels in the absence of magnetic field

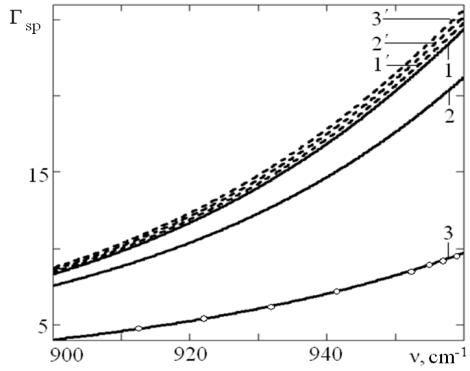

Fig. 5. SP damping coefficient as function of frequency, $\Gamma_{sp}(n)$, in 6H-SiC: 1–sample ПСЕ-3Б; 2–sample SiC-1; 3–sample SiC-2; 1′−3′ (sample ПСЕ-3Б) – H = 30, 65, 100 kOe.

according to procedure described in [7]. The curves 1′−3′ present the $\Gamma_{sp}(\nu)$ dependence for the sample ПСЕ-3Б placed in magnetic field (30 (1′), 65 (2′) and 100 (3′) kOe) at orientation $\vec{H} \perp K$, $\vec{H}$‖y .

Several mechanisms of SP damping may be found in literature. In particular, energy may be transferred from SPS to bulk plasmon via surface scattering of electrons owing to not too deep penetration of light and presence of a depleted layer at the surface. The above factors can favor energy transfer [7, 13].

Table 3

Half-width of minimum in the ATR spectrum, Γ_p, and SP damping coefficient, Γ_{sp}, in 6H-SiC single crystal at $H = 0$ and 100 kOe.

φ, °	H = 0				H = 100 kOe			
	ν_{min} (cm^{-1})	χ	Γ_p (cm^{-1})	Γ_{sp} (cm^{-1})	ν_{min} (cm^{-1})	χ	Γ_p (cm^{-1})	Γ_{sp} (cm^{-1})
C‖x								
ПСЕ – 3Б ($\gamma_{p\perp} = 620\,\text{cm}^{-1}$, $\gamma_{p\parallel} = 340\,\text{cm}^{-1}$, $\gamma_{f\perp,\parallel} = 12\,\text{cm}^{-1}$)								
30	917	1.398	29	22	917	1.398	29	22
35	937	1.691	188	171	937	1.692	190	174
SC-1 ($\gamma_{p\perp} = 700\,\text{cm}^{-1}$, $\gamma_{p\parallel} = 260\,\text{cm}^{-1}$, $\gamma_{f\perp,\parallel} = 14\,\text{cm}^{-1}$)								
30	919	1.41	28	23	919	1.4	30	23
35	939	1.714	215	198	939	1.714	219	202
SC-2 ($\gamma_{p\perp} = 830\,\text{cm}^{-1}$, $\gamma_{p\parallel} = 450\,\text{cm}^{-1}$, $\gamma_{f\perp,\parallel} = 12\,\text{cm}^{-1}$)								
30	922	1.415	45	34	922	1.415	45.12	34
35	944	1.752	415	359	944	1.752	420.45	364
C‖z								
ПСЕ – 3Б ($\gamma_{p\perp} = 0$, $\gamma_{p\parallel} = 0$, $\gamma_{f\perp,\parallel} = 0$)								
30	933	1.41	134	97	933	1.41	139	115
SC-1 ($\gamma_{p\perp} = 0$, $\gamma_{p\parallel} = 0$, $\gamma_{f\perp,\parallel} = 0$)								
30	938	1.42	230	163	938	1.435	—	—
SC-2 ($\gamma_{p\perp} = 0$, $\gamma_{p\parallel} = 0$, $\gamma_{f\perp,\parallel} = 0$)								
30	946	1.34	157	94	946	1.35	—	204
35	956	1.39	252	165	956	1.43	—	—
50	958	1.4	327	203	958	1.46	—	—
C‖y								
ПСЕ – 3Б ($\gamma_{p\perp} = 0$, $\gamma_{p\parallel} = 0$, $\gamma_{f\perp,\parallel} = 0$)								
30	945	1.425	274	180	945	1.42	296	180
35	963	1.594	—	437	963	1.59	—	473
SC-1 ($\gamma_{p\perp} = 0$, $\gamma_{p\parallel} = 0$, $\gamma_{f\perp,\parallel} = 0$)								
30	954	1.445	380	237	954	1.594	402	245
SC-2 ($\gamma_{p\perp} = 0$, $\gamma_{p\parallel} = 0$, $\gamma_{f\perp,\parallel} = 0$)								
50	984	1.51	594	543	984	1.515	470	436

It follows from Fig. 5 that the SP damping coefficient decreases as the free charge carrier concentration in 6H-SiC single crystal grows. The reverse behavior vs observed at growth of magnetic field in which the semiconductor under investigation is placed.

The SP damping coefficient in 6H-SiC single crystal was obtained with graphical technique [7] for the samples SC-1, SC-2 and ПСЕ-3Б at magnetic fields of 0, 30, 65 and 100 kOe and orientations C‖y, $K \perp C$, xy‖C; C‖z, $K \perp C$, $xy \perp C$; C‖x, K‖C, xy‖C, $\vec{H} \perp K$, $\vec{H}$‖y (see Table 3).

Conclusion

Thus, in this work, for the first time, the ATR spectra were detected in the region of excitation of surface plasmon-phonon polaritons in uniaxial hexagonal 6H-SiC single crystal placed in a strong uniform magnetic field. We studied the dispersion dependences and damping coefficients of surface plasmon-phonon and phonon polaritons in 6H-SiC single crystal placed in a strong uniform magnetic field. It is shown that new dispersion branches appear in 6H-SiC because of magnetic field action. The number of these branches

depends on the optical and electrophysical parameters of the crystal studied as well as its orientation and magnetic field strength. A dependence of SP damping coefficient on the strength of external magnetic field was found. However, the mechanism of this dependence needs further investigation.

Венгер Є.Ф. – доктор фізико-математичних наук, професор, член-кор. НАН України;
Мельничук О.В. – доктор фізико-математичних наук, професор, проректор з наукової роботи та міжнародних зв'язків, завідувач кафедри фізики;
Мельничук Л.Ю. – кандидат фізико-математичних наук, доцент кафедри фізики;
Євтушенко А.І. – асистент кафедри фізики.

[1] V.I. Al'shits and V.N. Lyubimov. Dispersionless surface polaritons in the vicinity of different sections of optically uniaxial crystals // *Fiz. Tverd. Tela,* **44**(2), pp. 371-374 (2002).
[2] E. A. Vinogradov. Semiconductor microcavity polaritons // *Uspekhi Fiz. Nauk,* 172(12), pp. 1371-1410 (2002).
[3] V. N. Datsko and A. A. Kopylov. On electromagnetic surface waves // *Uspekhi Fiz. Nauk,* **178**(1), pp. 109-110 (2008).
[4] N. P. Stepanov. Plasmon-phonon-polaritons in bismuth−antimony crystals doped with an acceptor impurity // *Fiz. Tekh. Poluprov,* **38**(5), pp. 552-555 (2004).
[5] A. N. Furs and L. M. Barkovskii. Surface electromagnetic waves in Faraday media // *Zh. Tekh. Fiz.*, **73**(4), pp. 9-16 (2003).
[6] Peter F., Tsunenobu K., Lothar L., and Gerhard P. Silicon Carbide: Growth, Defects, and Novel Applications, Vol. 1, 528 p. (2009); Power Devices and Sensors, Vol. 2, 520 p. (2009).
[7] E. F. Venger, O. V. Melnichuk, and Yu. A. Pasechnik. *Residual Rays Spectroscopy.* Naukova Dumka, Kyiv. 191 p. (2001).
[8] A. V. Melnichuk and Yu. A. Pasechnik. Anisotropy of the effective mass of electrons in silicon carbide // *Fiz. Tverd. Tela,* **34**(2), pp. 423-428 (1992).
[9] A. V. Melnichuk. Study of surface plasmon-phonon polaritons in single crystals SiC-6H by ATR // *Poverkhnost'. Fizika, Khimiya, Mekhanika,* (7), pp. 76-81 (1998).
[10] E. F. Venger, L. Ju. Melnichuk, O. V. Melnichuk et al. Surface plasmon-phonon polaritons in silicon carbide // *Ukr. Fiz. Zh.*, **43**(5), pp. 598-603 (1998).
[11] A. V. Melnichuk and Yu. A. Pasechnik. Influence of anisotropy on the dispersion of surface plasmon-phonon polaritons in silicon carbide // *Fiz. Tverd. Tela,* **40**(4), pp. 636-639 (1998).
[12] E. F. Venger, A. I. Evtushenko, L. Yu. Melnichuk, and A. V Melnichuk. Reflectance spectra of a 6H-SiC single crystal placed in a strong homogeneous magnetic field // *Journal of Engineering Physics and Thermophysics,* **82**(6), pp. 1211-1218 (2009) (E-mail: http://www.springerlink. com/content/4043151v3243r701).
[13] V. M. Agranovich and D. L. Mills (eds.). Surface Polaritons: Electromagnetic Waves at Surfaces and Interfaces. *Amsterdam: North-Holland.* 528 p. (1982).
[14] A. V. Melnichuk and Yu. A. Pasechnik. Attenuation of surface plasmon-phonon polaritons in zinc oxide // *Fiz. Tverd. Tela,* **38**(8), pp. 2343-2346 (1996).
[15] E. F. Venger, A. V. Melnichuk, L. Ju. Melnichuk, and Ju. A. Pasechnik. Anisotropy of the ZnO Single Crystal Reflectivity in the Region of Residual Rays // *Phys. Status Solidi (b),* **188**(2), pp. 823-831 (1995).

Є.Ф. Венгер[1], А.І. Євтушенко[2], Л.Ю. Мельничук[2], О.В. Мельничук[2]

Поверхневі поляритони в монокристалах 6H-SiC, розміщених у сильному однорідному магнітному полі

[1]Інститут фізики напівпровідників імені В.Є. Лашкарьова НАН України, Київ, Україна, 03028, проспект Науки, 41, м. Київ 28, e-mail: venger@isp.kiev.ua
[2]Ніжинський державний університет імені Миколи Гоголя, Україна, 16600, вул. Кропив'янського, 2, м. Ніжин; e-mail: mov310@mail.ru.

Показано можливість збудження поверхневих фононних та плазмон-фононних поляритонів (ПП) в оптично-анізотропних монокристалах карбіду кремнію (політип 6H), розміщених у сильному однорідному магнітному полі за взаємно-ортогональних орієнтацій оптичної осі, хвильового вектора та магнітного поля: $C\|x$, $K\|C$, $xy\|C$; $C\|z$, $K \perp C$, $xy \perp C$; $C\|y$, $K \perp C$, $xy\|C$, $\vec{H} \perp K$, $\vec{H}\|y$. Зареєстровано спектри порушеного повного внутрішнього відбивання (ППВВ) та досліджено основні властивості ПП (дисперсійні криві та коефіцієнт затухання ПП) при дії на монокристал 6H-SiC сильного однорідного магнітного поля. Виявлено вплив однорідного магнітного поля на властивості ПП 6H-SiC.

Ключові слова: поверхневі поляритони, анізотропія, магнітне поле, дисперсійні криві, карбід кремнію.